NUSC Technical Report 6772
1 November 1989

(4)

Underwater Acoustic Scattering from Spherical Particulates and Bubbles

K. B. Sullivan-Silva
Weapon Systems Technology and Assessment Department

Naval Underwater Systems Center
Newport, Rhode Island / New London, Connecticut

4

PREFACE

This technical effort was performed under the NUSC Bid and Proposal (B&P) Program as part of the B&P project "Effect of Ocean Medium Fluctuations on ASW Systems," Job Order 782P13, principal investigator K.B. Sullivan-Silva (Code 8213), senior advisor L. Goodman (Code 8212). The B&P Program provides funding for preliminary, conceptual, and technical work necessary for the generation of complete and comprehensive proposals for direct-funded work.

The technical reviewer for this report was L. Goodman (Code 8212).

REVIEWED AND APPROVED: 1 NOVEMBER 1989

S. Mneek for

F.L. White
Head, Weapon Systems Technology
and Assessment Department

REPORT DOCUMENTATION PAGE

Form Approved
OMB No. 0704-0188

1. AGENCY USE ONLY (Leave blank)	2. REPORT DATE	3. REPORT TYPE AND DATES COVERED
	1 November 1989	Final

4. TITLE AND SUBTITLE

Underwater Acoustic Scattering from Spherical Particulates and Bubbles

5. FUNDING NUMBERS

782P13

6. AUTHOR(S)

K.B. Sullivan-Silva

7. PERFORMING ORGANIZATION NAME(S) AND ADDRESS(ES)

Naval Underwater Systems Center
Newport Laboratory
Newport, RI 02841-5047

8. PERFORMING ORGANIZATION REPORT NUMBER

TR 6772

9. SPONSORING/MONITORING AGENCY NAME(S) AND ADDRESS(ES)

10. SPONSORING/MONITORING AGENCY REPORT NUMBER

11. SUPPLEMENTARY NOTES

12a. DISTRIBUTION/AVAILABILITY STATEMENT

Approved for public release; distribution unlimited.

12b. DISTRIBUTION CODE

13. ABSTRACT *(Maximum 200 words)*

High frequency underwater acoustic scattering from spherical particulates is examined theoretically for purposes of comparison with available data to develop conclusions on the types and magnitudes of scattering in various geographical regions. The simplifying assumptions of an ideal fluid sphere and isotropic medium conditions are employed in the derivation of the theoretical particulate scattering model. This theory is detailed here and also presented in the form of scattering plots generated by a computer model developed in this study to facilitate accurate analysis of individual scatterers. Special theoretical cases are presented and examined, including those of a large sphere, a small sphere, a rigid sphere (highly incompressible), and a gas bubble (highly compressible), for which additional consideration of damping effects is provided.

14. SUBJECT TERMS

Underwater Acoustics
Acoustic Scattering

15. NUMBER OF PAGES

55

16. PRICE CODE

17. SECURITY CLASSIFICATION OF REPORT	18. SECURITY CLASSIFICATION OF THIS PAGE	19. SECURITY CLASSIFICATION OF ABSTRACT	20. LIMITATION OF ABSTRACT
UNCLASSIFIED	UNCLASSIFIED	UNCLASSIFIED	SAR

TABLE OF CONTENTS

LIST OF ILLUSTRATIONS*

*Figures 2 through 8 were generated via the computer model developed for this project.

UNDERWATER ACOUSTIC SCATTERING FROM SPHERICAL PARTICULATES AND BUBBLES

1. INTRODUCTION

The scattering of underwater sound is determined not only by the medium or environment through which the sound is propagating, but also by the nature of the acoustic target. Therefore, sound scattering in an ambient ocean volume can be modeled as being due to both particulate scatterers and medium fluctuations or turbulence. A comparative analysis of scattering theory and experimental data for both particulates and medium fluctuations would contribute to the development of successful underwater acoustic scattering models. As the initial step in examining these two categories of acoustic scatterers, this report provides an extensive review of the theory of scattering from spherical particulates, and analysis of this type of scattering via a computer model developed for this work.

Particulate scattering for this study was defined as the scattering of incident acoustic energy by particulates in the ocean. Particulates include those physical targets existing in the ocean volume, such as plant and animal life and debris, and nonliving targets such as bubbles and sand particles. Throughout the ocean these scatterers vary in size and density, thereby providing different amounts of interference to propagating acoustic energy. For ease in analysis and to provide the most general case, scattering by particulates is approximated by looking at scattering from individual spheres, of various sizes, densities, and indexes of refraction. The spherical or simple source model is generally used for studying the scattering patterns of acoustically small marine particulates (Rayleigh scatterers), since this model has been found to produce fairly accurate scattering patterns and simplifies the analysis (reference 1). The spherical model allows more direct assessment of scattering dependence on sound frequency, scatterer size, and compressibility, and allows a broader range of values and conditions to be examined, providing "ideal" values against which experimental data can be compared.

To examine quantitatively the scattering caused by these spherical particulates, the parameter of primary interest is the total scattering cross section σ_{total}, which represents the size of a particle necessary to intercept fully an amount of incoming power equal to the total power actually scattered by the given particle. This definition is based on the fact that while the total power scattered off the sphere is equal to the power

actually incident on or intercepted by the sphere, this amount does not necessarily equal the geometric (or potential incident) power, which is the product of the incident intensity and the geometric cross-sectional area of the sphere. The total scattering cross section, therefore, may be greater or less than the geometric cross-sectional area, depending on the properties of the scatterer. This "normalized" form of the scatterer size then allows focus on its sound scattering potential and demonstrates how the particle can behave like an acoustic target larger or smaller than it actually is.

In deriving the general form of the total scattering cross section for a sphere, acoustic radius (wavenumber x sphere radius), density, and index of refraction are the governing physical parameters. By applying a range of values for these variables, various scatterer cases are examined for σ_{total}: large to small rigid spheres and large to small fluid spheres. Limiting cases are also examined for the very rigid scatterer and the very fluid scatterer (gas bubble). While the given spherical particulate model applies over the range of these cases, special consideration of damping and resonance effects is also included for the gas bubble. However, to determine the total scattering cross section, or any other scattering parameter of interest, it is first necessary to derive a general equation for the pressure of the scattered acoustic wave at range r from the sphere center. Having this, it is then possible to examine the energy levels, scattering directions, etc., for a specified model. The detailed derivation of the general equation for the acoustic pressure of the scattered signal is presented below.

As shown in figure 1, acoustic energy travels in the form of a pressure wave of assumed amplitude P_{inc} and angular frequency ω. The motion of this wave occurs in the ocean medium of known density ρ and sound speed c. For simplicity, straight-line geometric acoustics is assumed for propagation through the medium. As the energy strikes a small spherical target a large distance from its source, the pressure wave is approximately a plane wave striking a target of geometric cross section πa^2, where a is the sphere radius. The incident plane wave then induces an energy wave within the sphere (range $r < a$) and an external spherically propagating wave ($r > a$). By applying a three-dimensional coordinate system to this model, the incident wave is assumed to approach the sphere along the z axis and, by spherical symmetry, the dependence on spherical angle ϕ is eliminated. After applying equilibrium relations for pressure and radial particle velocity at the interface between the sphere surface and the surrounding medium ($r = a$), the following two boundary conditions exist (reference 2):

1. Continuity of Pressure at Sphere Boundary:

$$P_{inc}(a) + P_{sc}(a) = P_{int}(a) \ , \qquad (1)$$

2. Continuity of Radial Velocity at Sphere Boundary:

$$u_{inc}(a) + u_{sc}(a) = u_{int}(a) \ . \qquad (2)$$

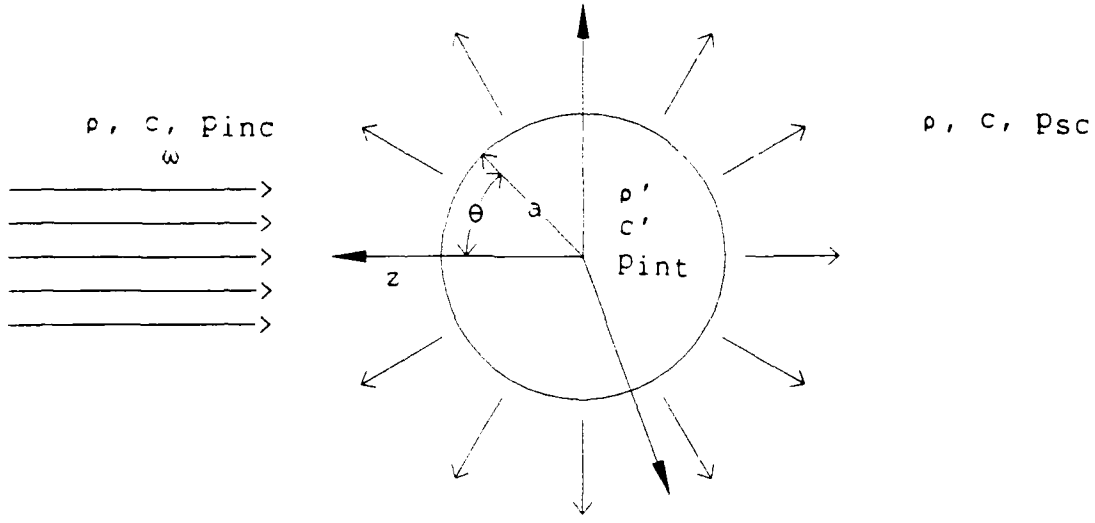

INCIDENT PLANE WAVE PARAMETERS (z AXIS)	INTERIOR (SPHERE) WAVE PARAMETERS (r < a)	SCATTERED PRESSURE WAVE PARAMETERS (r > a)
ρ = DENSITY	ρ' = DENSITY	(SAME ρ, c AS INCIDENT WAVE)
c = SOUND VELOCITY	c' = SOUND VELOCITY	
κ = WAVENUMBER	κ' = WAVENUMBER	
ω = ANGULAR FREQUENCY	a = SPHERE RADIUS	r = RANGE
P_{inc} = PRESSURE	p_{int} = PRESSURE	p_{sc} = PRESSURE
P_{inc} = PRESSURE AMPLITUDE	P_{int} = PRESSURE AMPLITUDE	P_{sc} = PRESSURE AMPLITUDE
u_{inc} = RADIAL VELOCITY	u_{int} = RADIAL VELOCITY	u_{sc} = RADIAL VELOCITY

Figure 1. General Model for Acoustic Scattering from a Sphere

2. CONTINUITY OF PRESSURE ANALYSIS

To apply the continuity of pressure relation at the sphere boundary, it is necessary to derive the wave pressure for each component. The three-dimensional wave equation is used for this purpose:

$$\nabla^2 p = (1/c^2)(\partial^2 p/\partial t^2) \ ,$$

where ∇ is the del operator, and t is the time.

Expanding this equation and putting it into spherical coordinates (neglecting dependence on angle ϕ due to symmetry) yields

$$\frac{1}{r^2}\frac{\partial}{\partial r}\left(r^2\frac{\partial p}{\partial r}\right) + \frac{1}{r^2 \sin\theta}\frac{\partial}{\partial \theta}\left(\sin\theta\,\frac{\partial p}{\partial \theta}\right) = \frac{1}{c^2}\frac{\partial^2 p}{\partial t^2} \ . \qquad (3)$$

By recognizing the pressure dependence on spherical coordinates r and θ and on time t, a general form of the pressure solution can be assumed

$$p = H(r)P(\theta)T(t) \ .$$

If one assumes a sinusoidal waveform for T(t), related to the pressure wave's compressions and rarefactions, this equation can be further specified as

$$p = H(r)P(\theta)\exp(-\imath\omega t) \ . \qquad (4)$$

Substituting this solution for p into the wave equation (3) and applying the method of separation of variables yields (reference 3)

$$\frac{1}{r^2}\frac{\partial}{\partial r}\left(r^2 P e^{-\imath\omega t}\frac{\partial H}{\partial r}\right) + \frac{1}{r^2 \sin\theta}\frac{\partial}{\partial \theta}\left(\sin\theta\, H e^{-\imath\omega t}\frac{\partial P}{\partial \theta}\right) = \frac{1}{c^2} HP \frac{\partial^2 e^{-\imath\omega t}}{\partial t^2};$$

dividing by $e^{-i\omega t}$ gives

$$\frac{1}{r^2}\frac{\partial}{\partial r}\left(r^2 P \frac{\partial H}{\partial r}\right) + \frac{1}{r^2 \sin\theta}\frac{\partial}{\partial \theta}\left(\sin\theta\, H \frac{\partial P}{\partial \theta}\right) = \frac{1}{c^2} HP(-i\omega)^2 \ ;$$

and dividing by PH gives

$$\frac{1}{Hr^2}\frac{\partial}{\partial r}\left(r^2 \frac{\partial H}{\partial r}\right) + \frac{1}{Pr^2 \sin\theta}\frac{\partial}{\partial \theta}\left(\sin\theta \frac{\partial P}{\partial \theta}\right) = -\frac{\omega^2}{c^2} \ .$$

Recognizing that wavenumber $\kappa = \omega/c$, and separating variables, one obtains

$$\frac{1}{H}\frac{\partial}{\partial r}\left(r^2 \frac{\partial H}{\partial r}\right) + \kappa^2 r^2 = -\frac{1}{P \sin\theta}\frac{\partial}{\partial \theta}\left(\sin\theta \frac{\partial P}{\partial \theta}\right) \ .$$

Since variables H(r) and P(θ) are completely separated, both sides of the equation are equal to the same constant D and can be solved as two separate equations:

$$-\frac{1}{P \sin\theta}\frac{d}{d\theta}\left(\sin\theta \frac{dP}{d\theta}\right) = D \ , \qquad (5)$$

$$\frac{1}{H}\frac{d}{dr}\left(r^2 \frac{dH}{dr}\right) + \kappa^2 r^2 = D \ . \qquad (6)$$

LEGENDRE FUNCTION

Examining equation (5) first, it is recognizable as a Legendre differential equation when rearranged with the following substitutions (reference 4):

$D = m(m + 1)$, where m = an integer ;

$x = \cos\theta$; therefore, $\sin^2\theta = 1 - x^2$, and $dx = -\sin\theta\, d\theta$.

By the chain rule,

$$\frac{d}{d\theta} = \frac{d}{dx}\frac{dx}{d\theta} = \frac{d}{dx}\frac{d(\cos\theta)}{d\theta} = -\sin\theta\frac{d}{dx} .$$

Substituting:

$$\frac{1}{\sin\theta}\left\{-\sin\theta\frac{d}{dx}\left[\sin\theta\left(-\sin\theta\frac{dP}{dx}\right)\right]\right\} + m(m + 1)P = 0 ,$$

$$-\frac{d}{dx}\left[(-1)\sin^2\theta\frac{dP}{dx}\right] + m(m + 1)P = 0 ,$$

$$\frac{d}{dx}\left(\sin^2\theta\frac{dP}{dx}\right) + m(m + 1)P = 0 ,$$

$$\frac{d}{dx}\left[(1 - x^2)\frac{dP}{dx}\right] + m(m + 1)P = 0 .$$

Expanding:

$$(-2x)\frac{dP}{dx} + (1 - x^2)\frac{d^2P}{dx^2} + m(m + 1)P = 0 .$$

Rearranging leads to the Legendre form:

$$(1 - x^2)\frac{d^2P}{dx^2} - (2x)\frac{dP}{dx} + m(m + 1)P = 0 . \qquad (7)$$

The solution of equation (7) is the Legendre polynomial of order m:

$$P = P_m(x) = P_m(\cos\theta) \ , \tag{8}$$

which is derived by setting P equal to a power series and solving by the power series method (references 3 and 4). The solution $P_m(x)$ is finite for the range $x = -1$ to $x = +1$ and has the following values for the first two orders of m (reference 4):

$$m = 0: \quad P_0(\cos\theta) = 1 \ ,$$

$$m = 1: \quad P_1(\cos\theta) = \cos\theta \ .$$

Further solutions are found by employing the recurrence relation (reference 4):

$$P_m(\cos\theta) = \frac{(2m-1)(\cos\theta)[P_{m-1}(\cos\theta)]-(m-1)[P_{m-2}(\cos\theta)]}{m} . \tag{9}$$

BESSEL FUNCTION

Looking back to equation (6), it can now be rearranged and recognized as a Bessel function by applying the following definitions:

$D = m(m + 1)$, where m = an integer; and $z = \kappa r$.

By the chain rule,

$$\frac{d}{dr} = \frac{d}{dz}\frac{dz}{dr} = \kappa \frac{d}{dz} \ .$$

Making the above substitutions into equation (6):

$$r^2 \frac{d^2H}{dr^2} + 2r \frac{dH}{dr} + [\kappa^2 r^2 - m(m+1)]H = 0 ,$$

$$r^2 \frac{d}{dr}\left(\frac{dH}{dz}\kappa\right) + 2r\left(\frac{dH}{dz}\kappa\right) + [\kappa^2 r^2 - m(m+1)]H = 0 ,$$

$$r^2\kappa \frac{d}{dz}\left(\kappa \frac{dH}{dz}\right) + 2r\kappa \frac{dH}{dz} + [\kappa^2 r^2 - m(m+1)]H = 0 ,$$

$$r^2\kappa^2 \frac{d^2H}{dz^2} + 2r\kappa \frac{dH}{dz} + [\kappa^2 r^2 - m(m+1)]H = 0 ,$$

$$z^2 \frac{d^2H}{dz^2} + 2z \frac{dH}{dz} + [z^2 - m(m+1)]H = 0 .$$

Rearranging leads to the Bessel form:

$$\frac{d^2H}{dz^2} + \frac{2}{z}\frac{dH}{dz} + \left[1 - \frac{m(m+1)}{z^2}\right]H = 0 . \qquad (10)$$

The solution of this equation is the spherical Hankel function, which is valid for waves radiating outward into an unbounded medium (and is therefore infinite at r = 0 (reference 5)), and is comprised of the spherical Bessel function j_m (real part of the Hankel function) and the spherical Neumann function n_m (imaginary part of Hankel function). The solution $H_m(\kappa r)$ of the Bessel equation is therefore

$$H = H_m(\kappa r) = \begin{Bmatrix} j_m(\kappa r) \\ n_m(\kappa r) \end{Bmatrix} . \qquad (11)$$

The spherical Bessel and Neumann functions are sinusoidal functions of the product of the medium wavenumber κ and the distance from the sphere center r. As the real part of the Hankel

function, the spherical Bessel function j_m is finite at r = 0 and, therefore, is a solution for that point. However, the spherical Neumann function n_m is infinite at r = 0 and, therefore, is not a solution for the interior of the sphere (reference 5). The function values are as follows for the first two orders of m (reference 4):

$$m = 0: \quad j_0(\kappa r) = \sin(\kappa r)/(\kappa r) ,$$

$$n_0(\kappa r) = -\cos(\kappa r)/(\kappa r) ;$$

$$m = 1: \quad j_1(\kappa r) = \sin(\kappa r)/(\kappa r)^2 - \cos(\kappa r)/(\kappa r) ,$$

$$n_1(\kappa r) = -\cos(\kappa r)/(\kappa r)^2 - \sin(\kappa r)/(\kappa r) .$$

Further solutions can be found with the use of the recurrence relations (reference 4):

$$j_m(\kappa r) = \frac{2m-1}{(\kappa r)} j_{m-1}(\kappa r) - [j_{m-2}(\kappa r)] ,$$

$$n_m(\kappa r) = \frac{2m-1}{(\kappa r)} n_{m-1}(\kappa r) - [n_{m-2}(\kappa r)] . \qquad (12)$$

Putting the general solution forms (equations (8) and (11) for the pressure constituent functions back into the general pressure equation (4) yields a general solution form for the acoustic pressure p at range r from the sphere center (reference 2):

$$p = \sum_{m=0}^{\infty} A_m P_m(\cos\theta)[j_m(\kappa r) + \imath n_m(\kappa r)]e^{-\imath\omega t} , \qquad (13)$$

where A_m represents unknown constant coefficients.

This general solution for pressure p can be examined with respect to each component of the previously stated boundary condition (1), recognizing the limited applicability of the spherical Neumann function as a solution. Examining the incident acoustic wave first, it is noted that the spherical Neumann

function is valid only outside of the scattering sphere, taking on an infinite value at r = 0. This limitation affects the incident pressure wave solution since the incident wave is the total wave solution without scatterer interference, and thereby must be finite in value at r = 0 (reference 5). (This limiting condition of the spherical Neumann function will also affect the solution for the interior scattered wave (r < a).) This results in the incident pressure wave equation:

$$p = P_{inc} \sum_{m=0}^{\infty} F_m P_m(\cos\theta) j_m(\kappa r) e^{-\imath\omega t} \quad , \tag{14}$$

where F_m represents unknown constant coefficients.

The values of the constant coefficients F_m are determined by application of the Rayleigh equation and orthogonality of the Legendre function P_m (see the derivation of F_m in the appendix):

$$F_m = (-\imath)^m(2m + 1) \quad .$$

The incident wave pressure now becomes:

$$p_{inc} = P_{inc} \sum_{m=0}^{\infty} (-\imath)^m(2m + 1) P_m(\cos\theta) j_m(\kappa r) e^{-\imath\omega t} \quad . \tag{15}$$

For the scattered acoustic wave, the pressure solution represents an outwardly propagating spherical wave (r > a) and is a function of both the spherical Bessel and Neumann functions:

$$p_{sc} = \sum_{m=0}^{\infty} A_m P_m(\cos\theta)[j_m(\kappa r) + \imath n_m(\kappa r)] e^{-\imath\omega t} \quad . \tag{16}$$

The interior acoustic wave pressure (r < a) solution incorporates the sphere parameters rather than those of the medium and, in addition, must neglect the spherical Neumann component since n diverges for the interior (nonspherical) flow (r = 0):

$$P_{int} = \sum_{m=0}^{\infty} B_m P_m(\cos\theta) j_m(\kappa' r) e^{-i\omega t} , \qquad (17)$$

where B_m represents unknown constant coefficients.

Having now determined the three separate pressure equations for incident, scattered, and interior pressures (equations (15), (16), and (17)), it is noted that there are two unknown constants A_m and B_m. (However, the constant A_m is the significant one here since it is the only one present in the scattered pressure equation.) To determine the value of A_m, the second boundary condition (2), which is based on the radial component of the particle velocity at the boundary $r = a$, must be considered.

3. CONTINUITY OF RADIAL VELOCITY ANALYSIS

To employ the continuity of radial velocity boundary condition (equation (2)), it is necessary to define the radial velocity equations. These are derived from the governing relationship between radial velocity and pressure (reference 4):

$$u = (-\imath/\rho c)[\partial p/\partial(\kappa r)] \ , \tag{18}$$

where u is the radial component of velocity, and the other variables are as defined previously in figure 1.

Applying this relation to the derived pressure equations for the incident (15), scattered (16) and interior (17) pressure waves leads to the radial velocity equation for each of the waves. It should be noted that, in taking the partial derivative of the pressure equation for each case, the only affected parameters are the spherical Bessel and Neumann functions, since they are the only portions of each equation dependent on the wavenumber (κ) and the range (r). Therefore, the three equations for radial velocity are as follows:

1. Incident Wave:

$$u_{inc} = \left(\frac{-\imath}{\rho c}\right) P_{inc} \sum_{m=0}^{\infty} (-\imath)^m P_m(\cos\theta)\alpha_m(\kappa r)e^{-\imath\omega t} \ , \tag{19}$$

where

$$\alpha_m(\kappa r) = (2m + 1)\{\partial[j_m(\kappa r)]/\partial(\kappa r)\} \ ,$$

$$= m j_{m-1}(\kappa r) - (m + 1) j_{m+1}(\kappa r) \ .$$

2. Scattered Wave (r > a):

$$u_{sc} = \left(\frac{-\imath}{\rho c}\right) \sum_{m=0}^{\infty} \frac{A_m}{(2m+1)} P_m(\cos\theta)[\alpha_m(\kappa r) + \imath\beta_m(\kappa r)]e^{-\imath\omega t} \ , \tag{20}$$

where

$$\beta_m(\kappa r) = (2m + 1)\{\partial[n_m(\kappa r)]/\partial(\kappa r)\} ,$$

$$= m n_{m-1}(\kappa r) - (m + 1) n_{m+1}(\kappa r) .$$

3. Interior Wave ($r < a$):

$$u_{int} = \left(\frac{-\imath}{\rho' c'}\right) \sum_{m=0}^{\infty} \frac{B_m}{(2m+1)} P_m(\cos\theta)\alpha_m(\kappa' r) e^{-\imath\omega t} . \qquad (21)$$

As noted earlier, the two undefined constants A_m and B_m remain in the pressure and velocity equations. By substituting the separate wave equations for velocity (equations (19), (20), and (21)) into the radial velocity boundary condition (2), and the wave equations for pressure (equations (15), (16), and (17)) into the pressure boundary condition (1), two equations with two unknown constants are obtained. It is then possible to solve for the function A_m (reference 2):

$$A_m = -P_{inc}(-\imath)^m (2m + 1)/(1 + \imath C_m) ,$$

where

$$C_m = \frac{[\alpha_m(\kappa' a)/\alpha_m(\kappa a)][n_m(\kappa a)/j_m(\kappa' a)] - [\beta_m(\kappa a)/\alpha_m(\kappa a)]gh}{[\alpha_m(\kappa' a)/\alpha_m(\kappa a)][j_m(\kappa a)/j_m(\kappa' a)] - gh} , \qquad (22)$$

$$g = \rho'/\rho ,$$

and

$$h = c'/c .$$

Substituting this solution into the pressure equation (13) yields a general form for the pressure of the scattered acoustic wave at range r greater than the sphere radius a ($r > a$):

$$p_{sc} = -P_{inc} \sum_{m=0}^{\infty} (-\imath)^m \frac{(2m+1)}{(1+\imath C_m)} P_m(\cos\theta)[j_m(\kappa r) + \imath n_m(\kappa r)]e^{-\imath\omega t} .$$

An additional approximation is available for simplifying the spherical Bessel and Neumann functions for large distances r from the sphere ($r >> a$). When taken in the limit, these functions reduce to the following (references 2 and 4):

As κr approaches infinity,

$$\begin{aligned} j_m(\kappa r) &\longrightarrow (1/\kappa r)\cos[\kappa r - (m+1)\pi/2] , \\ n_m(\kappa r) &\longrightarrow (1/\kappa r)\sin[\kappa r - (m+1)\pi/2] . \end{aligned} \tag{23}$$

By substituting these solutions for j_m and n_m into the above equation for the scattered pressure p_{sc}, the final form for scattered pressure at a large distance r from the scattering sphere ($r >> a$) is derived as follows:

$$\begin{aligned} &(-\imath)^m[j_m(\kappa r) + \imath n_m(\kappa r)] \\ &= (-\imath)^m(1/\kappa r)\{\cos[\kappa r - (m+1)\pi/2] \\ &\quad + \imath\sin[\kappa r - (m+1)\pi/2]\} , \\ &= (-\imath)^m(1/\kappa r)e^{\{\imath[\kappa r-(m+1)\pi/2]\}} , \\ &= (-\imath)^m(1/\kappa r)e^{(\imath\kappa r)}e^{[-\imath(m+1)\pi/2]} , \\ &= (-\imath)^m(1/\kappa r)e^{(\imath\kappa r)}[e^{(-\imath\pi/2)}]^{m+1} . \end{aligned}$$

Using the definition $e^{(-\imath\pi/2)} = -\imath$,

$$\begin{aligned} &= (-\imath)^m(1/\kappa r)e^{(\imath\kappa r)}(-\imath)^{m+1} , \\ &= (-\imath)^{2m+1}(1/\kappa r)e^{(\imath\kappa r)} , \\ &= (-\imath)^{2m}(-\imath)^1(1/\kappa r)e^{(\imath\kappa r)} , \\ &= (-1)^m(-\imath)(1/\kappa r)e^{(\imath\kappa r)} . \end{aligned} \tag{24}$$

Therefore, using the above spherical Bessel and Neumann function limiting approximations, the scattered pressure p_{sc} at large distances from the sphere ($r >> a$) can be reduced to the following

equation (agreeing with that given by Anderson in reference 2):

$$P_{sc} = P_{inc}\frac{(\imath)}{(\kappa r)}e^{(\imath\kappa r-\imath\omega t)}\sum_{m=0}^{\infty} P_m(\cos\theta)(-1)^m\frac{(2m+1)}{(1+\imath C_m)} . \quad (25)$$

Equation (25) is the fundamental equation for the scattered pressure field at long range r from a sphere.

4. SCATTERING RELATIONS

Having a general form of the pressure equation for large distances r from the sphere, it is now possible to derive the relationships between geometric and scattered pressures, both total and as a function of direction, giving a measure of the magnitude of the acoustic scattering from a sphere. Using the variable notation of reference 2, one can define the normalized reflectivity R of a given sphere as the ratio of scattered to geometric pressure amplitudes in a specific scattering direction defined by angle θ, i.e.,

$$R = p_{sc} / p_{geom} \quad , \tag{26}$$

where p_{sc} is the actual scattered pressure amplitude in direction θ at range r, and p_{geom} is the geometric scattered pressure amplitude at range r.

The geometric scattered pressure amplitude is the theoretical value produced at range r when all the incoming energy is perfectly incident on the geometric cross section of the sphere and is scattered uniformly from the perfectly reflecting sphere. Therefore, the geometric scattered pressure amplitude can be derived from an equivalence between the incoming geometric power and the outgoing geometric power. Since by definition power equals intensity ($p^2/\rho c$) multiplied by area, and since the parameters of density and sound speed would be the same for the incoming and scattered waves (both in the same medium), this equivalence reduces to

$$(\text{Pressure}^2 * \text{Area})_{inc} = (\text{Pressure}^2 * \text{Area})_{geom} \ .$$

The scattering cross-sectional area for geometric scattering would be equal to the surface area of a sphere of radius r ($4\pi r^2$), while the geometric cross-sectional area for the incident plane wave is equal to the area of a plane cross section of a sphere, or the area of a circle of radius a (πa^2). Therefore, the equation for the geometric scattered pressure amplitude is as follows:

$$p_{geom} = P_{inc}(\pi a^2/4\pi r^2)^{\frac{1}{2}} = P_{inc}(a/2r) \ . \tag{27}$$

Using this relation and substituting the amplitude portion of the scattered pressure equation solved previously (25), the normalized

reflectivity can be written as

$$R = \frac{2}{\kappa a} \left| \sum_{m=0}^{\infty} P_m(\cos\theta)(-1)^m \frac{(2m+1)}{(1+\imath C_m)} \right| , \qquad (28)$$

where $P_m(\cos\theta)$ and C_m were defined earlier by equations (9) and (22), respectively. Expansion of the portion of the reflectivity equation within the absolute value or amplitude delimiters requires manipulation of the imaginary component $(1 + \imath C_m)$:

$$R = \frac{2}{\kappa a} \left| \sum_{m=0}^{\infty} P_m(\cos\theta)(-1)^m \frac{(2m+1)}{(1+\imath C_m)} \frac{(1-\imath C_m)}{(1-\imath C_m)} \right| ,$$

$$= \frac{2}{\kappa a} \left| \sum_{m=0}^{\infty} P_m(\cos\theta)(-1)^m \frac{(2m+1)\ (1-\imath C_m)}{(1+C_m^2)} \right| ,$$

$$= \frac{2}{\kappa a} \left[\left| \sum_{m=0}^{\infty} P_m(\cos\theta)(-1)^m \frac{(2m+1)}{(1+C_m^2)} \right.\right.$$

$$\left.\left. - \imath C_m \sum_{m=0}^{\infty} P_m(\cos\theta)(-1)^m \frac{(2m+1)}{(1+C_m^2)} \right| \right] ,$$

$$= (2/\kappa a)|x - \imath y| ,$$

$$= (2/\kappa a)(x^2 + y^2)^{\frac{1}{2}} ,$$

$$R = \frac{2}{\kappa a} \left\{ \left[\sum_{m=0}^{\infty} P_m(\cos\theta)(-1)^m \frac{(2m+1)}{(1+C_m^2)} \right]^2 \right.$$

$$\left. + \left[\sum_{m=0}^{\infty} P_m(\cos\theta)(-1)^m \frac{(2m+1)\ C_m}{(1+C_m^2)} \right]^2 \right\}^{\frac{1}{2}} . \qquad (29)$$

This value indicates the fraction of geometric energy incident on the sphere that is scattered off it in a particular

direction specified by angle θ. The reflectivity value is clearly a strong function of scattering angle θ, scattering not being uniform in all directions from a sphere. This variation as a function of direction is seen graphically in figure 2, which shows the polar representations of the reflectivity (and therefore scattering strengths) as a function of varying θ only, for specified input values (chosen to allow direct comparison with results given in reference 2). These graphs were generated via the computer program developed in connection with this study and are discussed more extensively in section 6 of this report.

For the special case of backscattering of acoustic energy (for which, according to this model, $\theta = 0°$), the Legendre function $P_m(\cos\theta)$ approaches a constant value of 1 when summed over all m summation values (see equation (9)). This simplifies the reflectivity equation to

$$R = \frac{2}{\kappa a}\left\{\left[\sum_{m=0}^{\infty}(-1)^m\frac{(2m+1)}{(1+C_m^2)}\right]^2 + \left[\sum_{m=0}^{\infty}(-1)^m\frac{(2m+1)\,C_m}{(1+C_m^2)}\right]^2\right\}^{\frac{1}{2}} . \qquad (30)$$

(reflectivity for backscattering, $\theta = 0°$)

Figures 3 and 4, generated via the computer program, demonstrate the behavior of the reflectivity as a function of variable density ratio g, sound speed ratio h, and acoustic radius κa only, with the angle θ held constant at 0°. Again, these results compare favorably with those given by Anderson in reference 2.

Another parameter of interest for characterizing the scattering properties of a sphere is the total scattering cross section. As defined earlier, σ_{total} is a measure of the total power scattered out of the geometric input (incident) power hitting the sphere, thereby defining the amount of energy removed by the scatterer (reference 2). It has units of area, indicating the cross-sectional size of the sphere necessary to intercept the full amount of the power actually scattered from it. Rather than being just a ratio of the pressure amplitudes (as is the reflectivity), the total scattering cross section is determined from the ratio of scattered power to geometric power, thereby incorporating consideration of sphere size.

By using the definitions of power = intensity x area, and

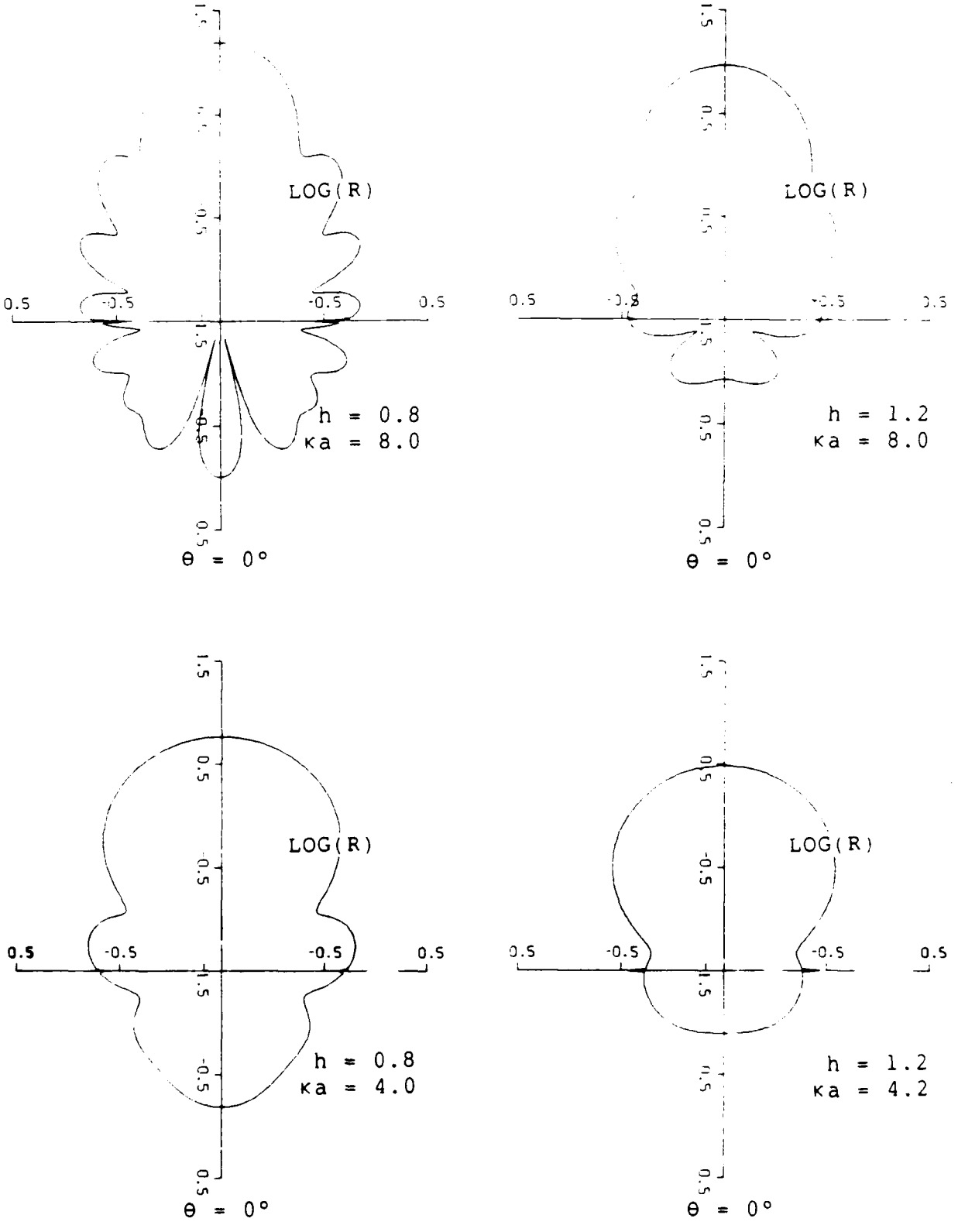

Figure 2. Reflectivity R for a Sphere as a Function of Angle θ (g = 1.0)

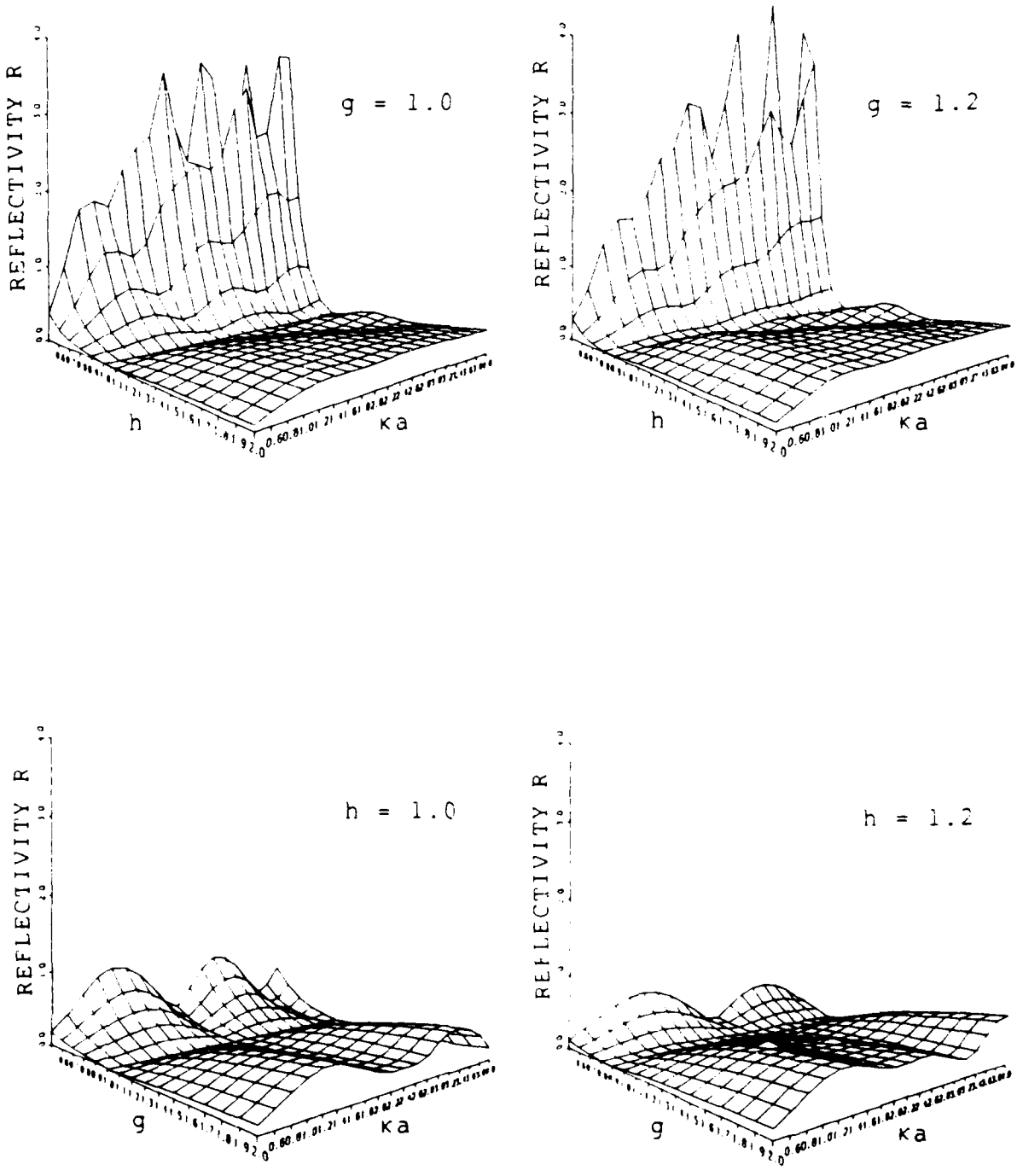

Figure 3. Backscattered Reflectivity R for a Sphere as a Function of Density Ratio g, Sound Speed Ratio h, and Wavenumber x Sphere Radius κa ($\theta = 0°$)

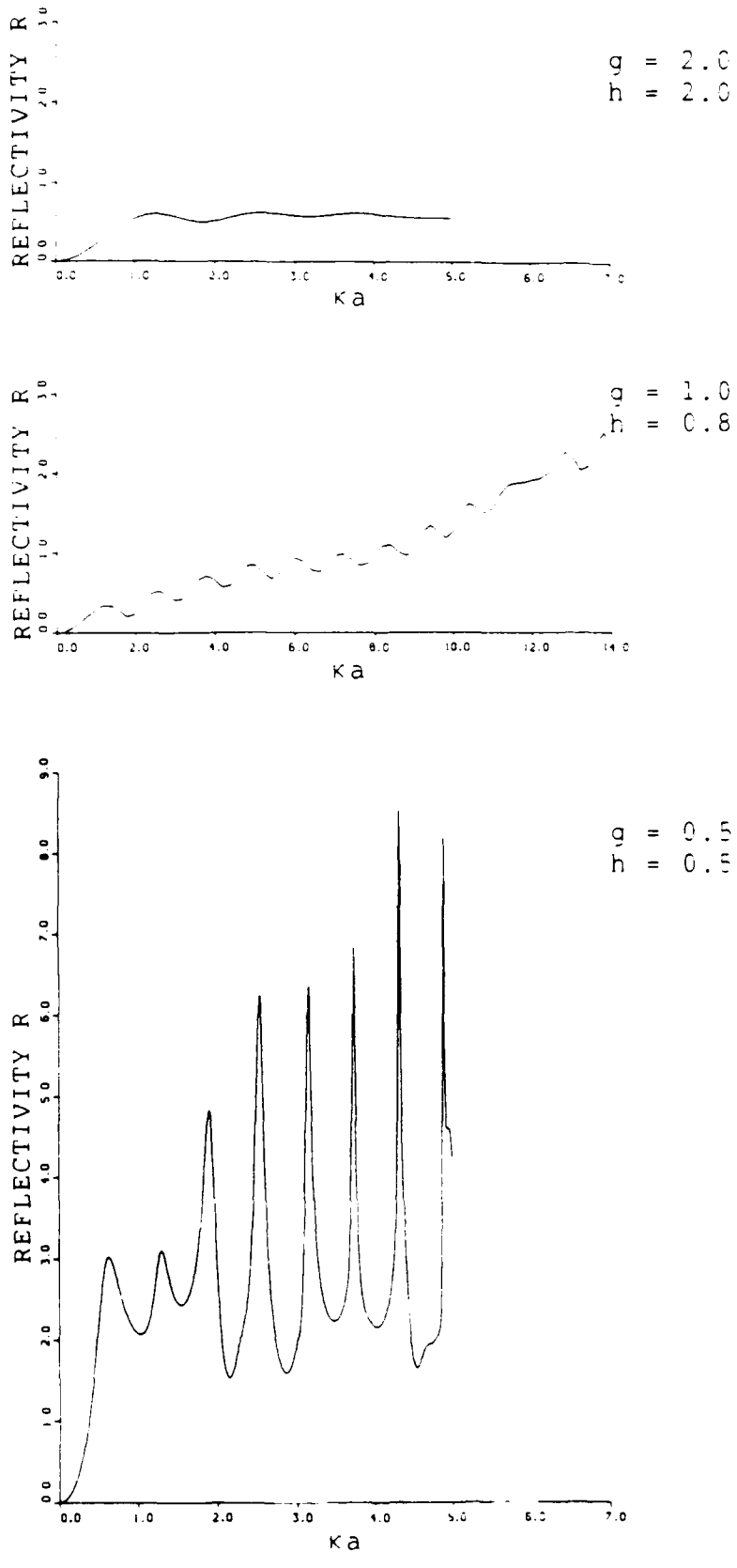

Figure 4. Backscattered Reflectivity R for a Sphere as a Function of Wavenumber x Sphere Radius Ka ($\theta = 0°$)

intensity = pressure^2/(density x sound speed), an interim power ratio Π can be calculated and used in the calculation of the scattering cross section:

$$\Pi = \frac{\text{Actual Scattered Power}}{\text{Geometrically Scattered Power}} ,$$

$$= \frac{(\text{Scattered Intensity x Scattered Area})}{(\text{Geometric Intensity x Geometric Area})} ,$$

$$= \frac{[(|p_{sc}|^2)/(\rho c)] \text{ x Scattered Area}}{[(|p_{geom}|^2)/(\rho c)] \text{ x } (4\pi r^2)} .$$

Noting that the density and sound speed are the same for incident and scattered energies, defining the actual scattered area as the integral taken over spherical surface s of radius r_o surrounding the scatterer (total surface area), and using the earlier equation for geometrically scattered power (27), one obtains

$$\Pi = \int_s |p_{sc}|^2 ds / P_{inc}^2 \pi a^2 . \qquad (31)$$

Expanding this equation with the derived solution for scattered pressure amplitude (from equation (25)) yields

$$\Pi = \frac{\int_s \left| P_{inc} \frac{\imath}{\kappa r} \sum_{m=0}^{\infty} P_m(\cos\theta)(-1)^m \frac{(2m+1)}{(1+\imath C_m)} \right|^2 ds}{P_{inc}^2 \pi a^2} . \qquad (32)$$

Defining the surface integral in spherical coordinates gives

$$\int_S ds = \int_S r^2 d\Omega = \int\int r^2 \sin\theta \, d\theta d\phi ,$$

where the radius parameter r is being held constant at r_o. Also, since angle ϕ varies from 0 to 2π radians, and since none of the equation components are functions of ϕ, the integral with respect

to angle ϕ can be performed, yielding a 2π factor in the remaining θ integrand. Squaring the terms in the numerator of equation (32) as indicated, recognizing that $|\imath| = 1$, and that angle θ varies from 0 to π radians then yields

$$\Pi = \int_0^{\pi} \left| \sum_{m=0}^{\infty} P_m(\cos\theta)(-1)^m \frac{(2m+1)}{(1+\imath C_m)} \right|^2 \frac{2\pi r_o^2 \sin\theta \, d\theta}{\pi a^2 \kappa^2 r_o^2} ,$$

$$= \int_0^{\pi} \sum_{m=0}^{\infty} P_m^2(\cos\theta) \frac{(2m+1)^2}{(1+C_m^2)} \frac{2\sin\theta}{\kappa^2 a^2} \, d\theta .$$

By letting $x = \cos\theta$, $dx = -\sin\theta \, d\theta$, and the new integrand limits become

$$x_1 = \cos\theta_1 = 1 , \quad \text{and} \quad x_2 = \cos\theta_2 = -1 ;$$

$$\Pi = - \int_{+1}^{-1} \sum_{m=0}^{\infty} P_m^2(x) \frac{(2m+1)^2}{(1+C_m^2)} \frac{2}{\kappa^2 a^2} \, dx .$$

Reversal of the order of the integrand limits is achieved by multiplying the integrand by -1:

$$\Pi = + \int_{-1}^{+1} \sum_{m=0}^{\infty} P_m^2(x) \frac{(2m+1)^2}{(1+C_m^2)} \frac{2}{\kappa^2 a^2} \, dx .$$

Rearranging yields

$$\Pi = + \frac{2}{\kappa^2 a^2} \sum_{m=0}^{\infty} \int_{-1}^{+1} P_m^2(x) dx \frac{(2m+1)^2}{(1+C_m^2)} .$$

The integral portion of this equation is now in the proper form for applying the Legendre principle of orthogonality (references 3 and 6), which yields a simple series substitution:

$$\int_{-1}^{+1} P_m^2(x)dx = \frac{2}{(2m+1)} . \tag{33}$$

Therefore, the simplified form of the power ratio Π now becomes

$$\Pi = \frac{2}{\kappa^2 a^2} \sum_{m=0}^{\infty} \frac{2}{(2m+1)} \frac{(2m+1)^2}{(1+C_m^2)} ,$$

$$= \frac{4}{\kappa^2 a^2} \sum_{m=0}^{\infty} \frac{(2m+1)}{(1+C_m^2)} . \tag{34}$$

Various sets of inputs were tested with this equation (via the computer program) and were found to agree well with Anderson's results (reference 2); graphs are shown in figure 5.

The power ratio Π is related to the total scattering cross section σ_{total} in that it is equal to σ_{total} divided by the geometric scattering cross section σ_{geom}, which for this spherical model is equal to πa^2:

$$\Pi = \frac{\sigma_{total}}{\sigma_{geom}} = \frac{\int \sigma_\theta d\theta}{\sigma_{geom}} . \tag{35}$$

In other words, Π is the power ratio defining the nonideal scattering of the sphere or the degree to which it deviates from being a perfect scatterer (i.e., if $\Pi = 1$, the scattering is perfectly uniform and all the energy in equals the geometric energy amount, which equals the energy out, and σ_{total} equals the actual (geometric) sphere cross-sectional area). Multiplying this ratio by the geometric cross-sectional area πa^2 modifies that sphere size to the size (σ_{total}) necessary to intercept the total energy scattered (or actual energy intercepted). This scattered energy amount, as discussed previously, can be more or less than the geometric incident energy, depending on the scatterer-to-medium parameters. Likewise, the total scattering cross section σ_{total} may be greater or less than the sphere geometric cross-sectional area, depending on the scattering conditions, i.e.,

$$\sigma_{total} = \Pi\pi a^2 .$$

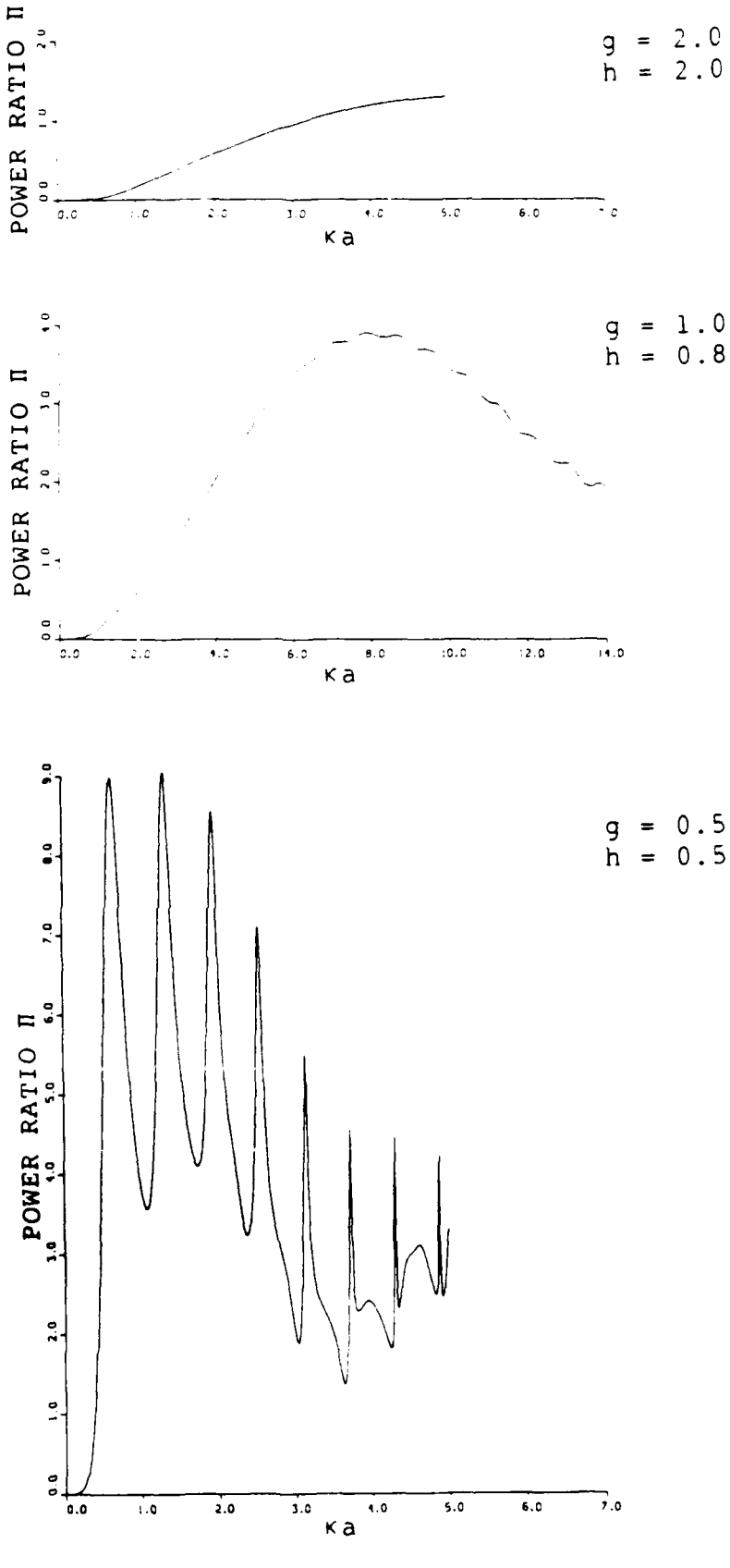

Figure 5. Scattered Power Ratio Π for a Sphere as a Function of Wavenumber x Sphere Radius Ka

Plots of the total scattering cross-section values for the same inputs used in figure 5 are provided in figure 6, again the difference being a factor of πa^2.

As mentioned previously, in connection with this study a computer program was developed to facilitate calculation of the scattering parameters for a sphere as a function of user-specified sphere and medium parameters. The computer model uses the complete theoretical scattering equations, incorporating both the spherical Bessel and Neumann functions, and the expanded Legendre function (equation (9)), with the only approximation employed being the simplified forms of j_m and n_m for a large scattering distance r from the sphere center (as shown in equations (23) and (24)). The close match of these computed results (figures 2 through 5) with Anderson's (see reference 2), in which approximations for Rayleigh and rigid-sphere scattering were employed (as discussed in the next section), verify the validity of the approximations (and likewise of the computer model) over the range tested. While the mathematical accuracy of the computer model was maximized through the use of the expanded spherical and Legendre functions, it must be remembered that this model (as was Anderson's) is somewhat limited through the assumptions of isotropy of sphere and medium parameters, etc., as specified earlier in the report. However, the model can be extremely valuable in studying acoustic scattering from marine particulates in that it shows the dependencies and trends of the scattering parameters with respect to scatterer size, compressibility, and sound frequency.

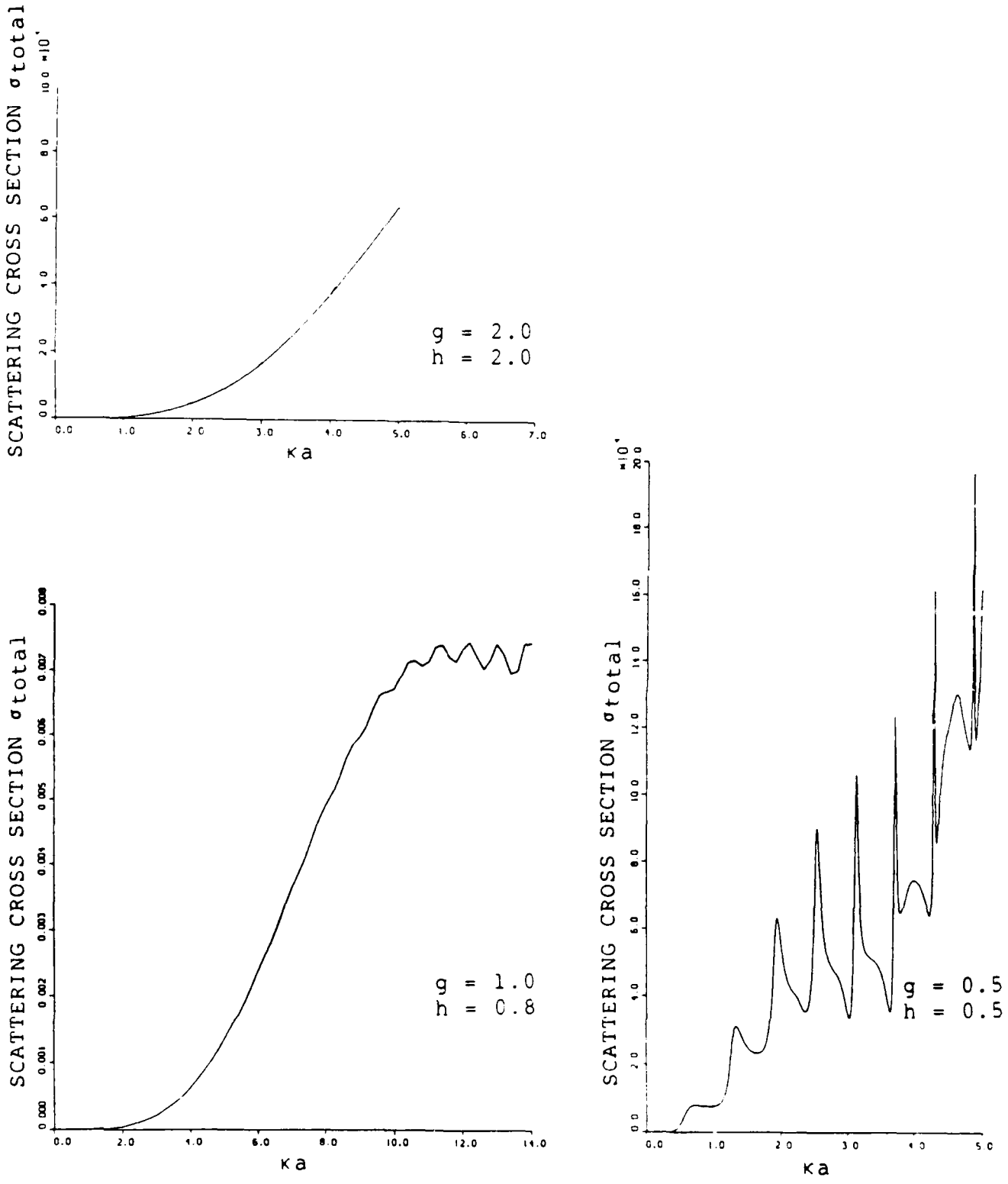

Figure 6. Total Scattering Cross Section σ_{total} for a Sphere as a Function of Wavenumber x Sphere Radius Ka

5. APPLICATIONS — LIMITING CASES

FIXED, RIGID SPHERE

In modeling a rigid sphere, the compressibility ($1/\rho c^2$) of the sphere is assumed to be much less than that of the surrounding fluid, such that the ratios of sphere-to-medium density g and sound velocity h are taken to approach infinity. This assumes almost perfect scattering of sound from the sphere surface (based on previous assumptions). This approximation can be used for both the large and small rigid sphere calculations. In addition, for the small sphere, the spherical Bessel and Neumann functions can be simplified by taking the limit as the sphere radius goes to zero; and, for the large sphere, the larger radius dominates the backscattering function solution.

The backscattering results generated by the spherical model are generally classified into two distinct categories in terms of response. The difference in the response type is determined by the size of the scatterer, with spheres of acoustic radius $\kappa a < 1$ producing Rayleigh scatter, and spheres of acoustic radius $\kappa a > 1$ producing geometric scatter (reference 1).

Rayleigh Scatter ($\kappa a << 1$)

When the size of the scattering sphere is much less than the sound wavelength λ ($2\pi a << \lambda$, therefore $\kappa a << 1$), certain simplifications of the scattering functions are possible. By letting the value of κa approach 0 in the limit, the spherical Bessel and Neumann functions can be simplified with the following known properties, since only the first terms in the series solutions remain critical (reference 4):

As κa approaches 0,

$$j_m(\kappa a) \longrightarrow (\kappa a)^m/[1 * 3 * 5 * \ldots * (2m + 1)] ,$$
$$n_m(\kappa a) \longrightarrow [-1 * 1 * 3 * 5 * \ldots * (2m - 1)]/(\kappa a)^{m+1} . \quad (36)$$

These relationships for scattering from very small spheres can then be used to determine the reflectivity ratio R. When applying the above conditions, the reflectivity equation for backscattering ($\theta = 0°$) for spheres of $\kappa a << 1$ becomes (reference 2):

$$R_{bs} = 2(\kappa a)^2 \left(\frac{1-gh^2}{3gh^2} + \frac{1-g}{1+2g} \right) , \qquad (\kappa a << 1) . \qquad (37)$$

Using this relationship, it can be seen that for a small, rigid sphere ($\kappa a << 1$, $g >> 1$, $h >> 1$), the square of the backscattering ratio (R_{bs}^2) is proportional to $(\kappa a)^4$, and therefore proportional to the frequency raised to the fourth power (ω^4). This has been shown graphically by Clay and Medwin (reference 1), defined in terms of a backscattering function ζ_{bs}. (The relationship between Clay and Medwin's ζ_{bs} and the reflectivity ratio R_{bs} used in this report is: $\zeta_{bs} = R_{bs}^2/4\pi$). It should be noted (and will be shown in a later figure), that for a small, rigid sphere, there is low backscatter. This is because the pressure waves tend to bend around the small sphere, rather than be reflected off of it (reference 1). It will also be shown that this relationship holds for values of κa up to $\kappa a \simeq 1$.

Geometric Scatter ($\kappa a >> 1$)

For values of $\kappa a \geq 1$, the backscattering response oscillates about and gradually converges to the ideal scattering value of $\zeta_{bs} = 1/4\pi$, or $R_{bs}^2 = 1$. As discussed previously, this ideal backscattering value of 1 represents complete reflection of all geometric power input; therefore, the total scattering cross section σ_{total} would be equal to the geometric (actual) sphere cross section. Since, for this case, the scattering parameters (R, Π, ζ) are functions of the geometric cross-sectional area of the sphere, this is called the region of geometric scattering response. (Initial oscillations of the backscattered response occur for $\kappa a > 1$ (see figure 7). These are due to diffraction effects or creeping waves at the sphere surface (reference 7)). Thus, the reflectivity ratio for backscattering (R_{bs}) for rigid spheres in the region of geometric scattering ($\kappa a >> 1$) is

$$R_{bs}^2 = 1 , \qquad (\kappa a >> 1) . \qquad (38)$$

As can be determined from the Rayleigh and Geometric backscattering approximations (equations (37) and (38)), the rigid sphere backscattering model acts as a highpass filter with the cutoff point at $\kappa a \simeq 1$ (reference 1).

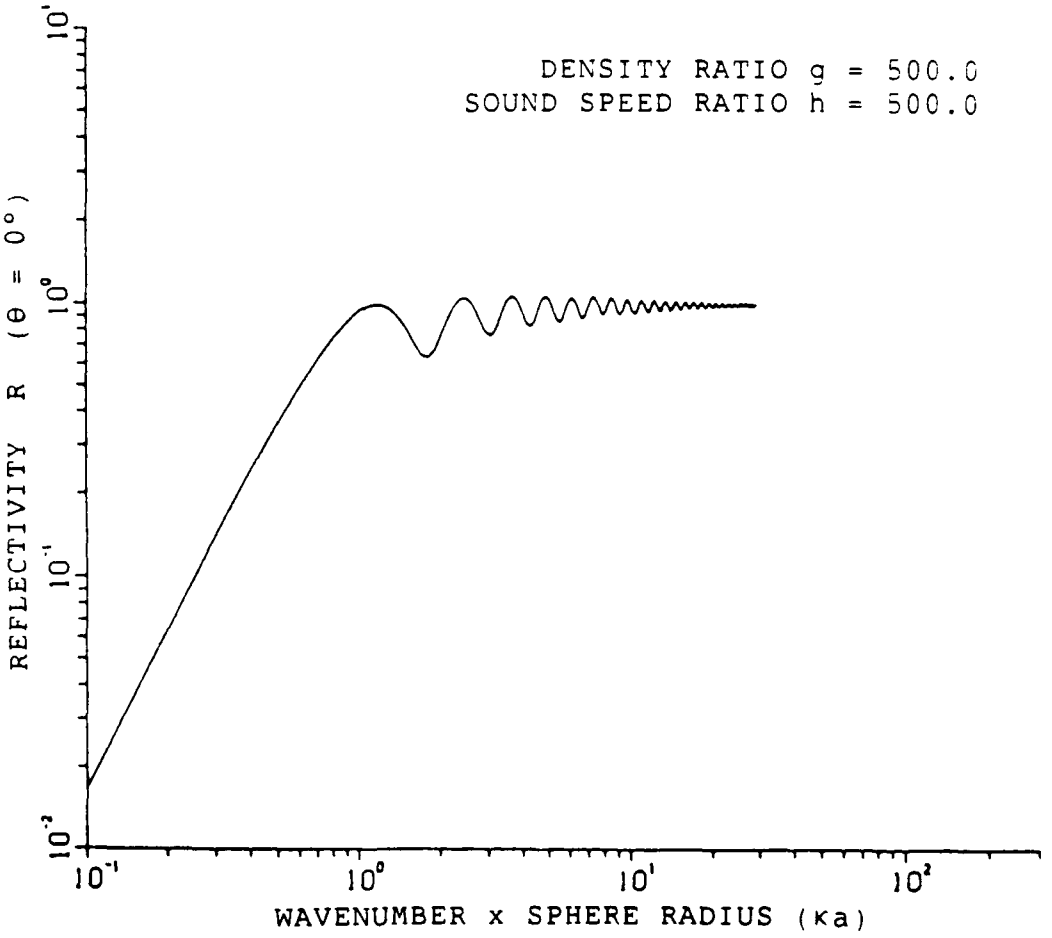

Figure 7. Backscattered Reflectivity R
for a Rigid Sphere (θ = 0°)

Rigid Sphere Model (g >> 1, h >> 1)

To further validate the accuracy of these (known) approximations and further test the computer model capabilities, the backscattering results for a rigid, nonresonant sphere, modeled by setting g >> 1 and h >> 1, were calculated via the computer program developed for this work (based on the expanded equations without the sphere size approximations). The results of this model test, for which density ratio g = 500.0 and sound speed ratio h = 500.0, are presented graphically in figure 7, and compare favorably with the results generated by Clay and Medwin using the Rayleigh and Geometric scatter approximations (reference 1). (Questions have arisen concerning application of the computer model for g and h values on the order of 10.0; "spikes" have been observed in some of the values for large κa (>10). It is not clear at this time whether these values indicate limitations in the model's applicability, or are true values representing the sphere's deviation from being a perfectly rigid scatterer at larger sizes, for certain g and h values. The apparent success of the model in examining the sphere of g and h = 500.0 would seem to support the latter possibility.)

FLUID, COMPRESSIBLE SPHERE

In modeling a fluid sphere, the compressibility ($1/\rho c^2$) of the sphere is assumed to be greater than that of the surrounding medium; therefore, the sphere-to-medium ratios of density g and sound speed h tend to be very small. This leads to a second important consideration, since the presence of interior waves and resonances becomes important for compressible spheres, in terms of both the magnitude and directions of the scattered energy. Detailed consideration of the sphere's interior resonance was simplified for the basic model derived in this work so far (further discussion of the generation of interior waves is found in section 6); also, analysis of damping factors was neglected. However, for the very fluid sphere, these concerns become more important and particularly so for the extreme fluid case of the gas bubble in water. In addition to being strong scatterers and absorbers of sound, bubbles can also affect the parameters of the surrounding medium, depending on the resonant conditions defined (reference 1). Because bubbles are so prevalent in water and have significant acoustic scattering capabilities, consideration of the bubble as an extreme fluid sphere case follows.

Fluid Sphere Model: Gas Bubble

As a special case of a fluid, highly compressible sphere, a gas bubble can be examined. Examination of the bubble as a scatterer of sound is a common and useful one since bubbles are so prevalent and powerful in terms of sound scattering in the ocean. Bubbles are generated on and beneath the surface by medium turbulence and waves, and exist as well in the form of the gas-filled swimbladders present in many kinds of fish. The strong effects that bubbles have on propagating sound in water are due to the difference in compressibilities of the two media involved and to the resonance characteristics of bubbles. When a gas bubble is insonified by a signal whose frequency is near to the bubble's resonant frequency, the bubble becomes a strong scatterer and absorber of sound waves (reference 1). Also, as already mentioned, bubbles can change the compressibility of the surrounding water, thereby affecting the speed of sound in the water.

While the spherical particulate model employed in this work so far applies to the fluid, compressible case (bubble), more complete analysis requires consideration of resonance and damping factors. The primary concern is the potential for a resonance scattering condition, which is dependent on the characteristic parameters of the target bubble (which in turn determine the bubble's natural frequency), and the frequency of the incident acoustic wave. A resonance condition is defined as occurring when the incident frequency of the system matches the natural frequency of the bubble, which is defined by the bubble compressibility and damping characteristics. This condition physically results in increasing (harmonic) oscillations of the bubble size, with the bubble pulsating and moving the surrounding liquid mass as it scatters the acoustic energy and converts some to heat. The magnitude of the oscillations is limited to a peak value, however, by various damping forces acting on the system, just as the magnitude of the scattered power (as a function of direction) and its effects on the surrounding medium are limited by absorption and other attenuating factors, all of which are among those parameters that need to be defined for the bubble.

Employing the same basic model for analysis as was used for the spherical particulate, the bubble can be modeled as a gas-filled sphere insonified by a planar acoustic wave, in an isotropic medium (water) of density ρ and sound speed c. The bubble is assumed to be much smaller than the incident wavelength ($a \ll \lambda$, $\kappa a \ll 1$), and it is not fixed in the medium. The pressure wave incident on the bubble surface generates waves inside the bubble that both absorb and rescatter energy. The scattered pressure wave can be assumed to be spherically

symmetrical, such that the bubble scattering pattern is omnidirectional (reference 1). Variables for the bubble model are defined as for the spherical particulate (figure 1), with conditions as follows:

1. Clean, free, spherical bubble; isotropic medium;
2. Bubble compressibility much greater than that of medium;
3. Energy: scattered, absorbed, converted to heat;
4. At resonance, incident frequency approximately equal to resonant frequency;
5. Surface tension effects - raise the resonant frequency;
6. Damping factors present (attenuation):
   - thermal conductivity - energy converted to heat;
   - shear viscosity absorption - increased damping;
   - reradiation of energy (spherical scattering);
7. Spherical symmetry in bubble wall motion and in scattering pattern.

Applying the equilibrium relations of continuity of pressure and radial velocity at the bubble-water interface gives the following boundary conditions (reference 1):

1. Continuity of Pressure at Bubble Boundary:

$$p_{inc}(a) + p_{sc}(a) + C_1\mu(u_{sc}/R) = p_{int}(a) , \quad (39)$$

2. Continuity of Radial Velocity at Bubble Boundary:

$$u_{sc}(a) = u_{int}(a) , \quad (40)$$

where C_1 is a dimensionless constant dependent on bubble geometry, μ is the dynamic coefficient of shear viscosity for water, R is the range from the bubble center (which is set equal to radius a), and u/R is the radial rate of strain.

The continuity equation for the acoustic pressure, as was the case for the particulate, defines the interior pressure wave acting on the inside of the bubble surface, opposed by both the incident and scattered pressure waves acting on the external surface of the bubble. In addition, for the bubble there is an external shear viscous force due to the stresses on the bubble surface, given by the quantity $C_1\mu(u/R)$.

The radial velocity continuity equation for the bubble (equation (40)) differs from that for the particulate in that there is no incident radial velocity component considered. This term is neglected because the incident radial velocity is much smaller than the interior radial velocity for a very compressible sphere. This can be recognized by looking at equation (18) for radial velocity. It is a function of the inverse of the product of density ρ and sound speed c. Therefore, for a very fluid sphere in the ocean, with $g << 1$ and $h << 1$, ρ and c of the sphere are very small and interior radial velocity is very large. For the medium, ρ and c are (comparatively) larger; therefore, incident radial velocity is much smaller. The magnitude of the scattered radial velocity is determined by the scattering conditions (g, h), and is therefore dependent on the interior radial velocity.

As was done with the particulate, it is useful to examine the scattering strength of a bubble in terms of its total scattering cross section σ_{total}. As derived in detail by Clay and Medwin (reference 1), and outlined in the appendix of this report, the equation for σ_{total} of a bubble is based on the ratio of scattered to incident powers:

$$\sigma_{total} = 4\pi R_1^2 \frac{|P_{sc}|^2}{|P_{inc}|^2} = \frac{4\pi a^2}{[(f_{res}/f_{inc})^2-1)]^2+\delta^2} \qquad (41)$$

where R_1 is a reference distance from the scatterer (= 1 m), fres is the resonant frequency of the bubble, f_{inc} is the frequency of incident wave, and δ is the damping parameter, defined as a function of thermal conductivity, reradiation, and shear viscosity. As mentioned, the background and derivation of this equation is provided in the appendix of this report; so analysis here will be limited to a brief discussion of the damping and resonance factors present.

Damping Constant δ. The damping constant δ is composed of three separate damping factors associated with shear viscosity,

thermal conductivity, and reradiation, i.e.,

$$\delta = \delta_{sv} + \delta_{tc} + \delta_r \ , \qquad (42)$$

where $\delta_{sv} = C_1\mu/(\rho\omega a^2)$ is the damping due to shear viscosity; $\delta_r = \kappa a$ is the damping due to reradiation; $\delta_{tc} = (d/b)(f_{res}/f_{inc})^2$ is the damping due to thermal conductivity; d/b is a damping variable incorporating thermal conductivity and specific heat values; and f_{res}/f_{inc} is the ratio of bubble resonant frequency to incident frequency, incorporating bubble physical parameters, surface tension, bubble depth, and incident wave considerations.

Resonance Frequency f_{res}. As mentioned previously, the resonant frequency is the parameter that largely dictates the magnitude of the scattering values generated. It describes the natural frequency of the bubble interior oscillations and includes the effects of surface tension and the non-adiabatic nature of the bubble oscillation process. The equation is presented here but is derived and presented as equation (A-16) in the appendix:

$$f_{res} = \frac{1}{2\pi a}\sqrt{\frac{3\beta\gamma b P_A}{\rho}} \ ,$$

where P_A is the ambient (external) pressure amplitude, b is the damping variable related to thermal conductivity, β is the damping variable related to surface tension effects, and γ is the ratio of constant-pressure to constant-volume specific heats.

As mentioned above, a detailed derivation of scattering from a gas bubble can be found in appendix A6 of reference 1. Also, a summary outline of the equations of interest is given in the appendix of this report; this is the analysis used in expanding the computer model to calculate scattering parameters for an insonified gas bubble.

A sample of the theoretical scattering analysis from a gas bubble is shown graphically in figure 8 (generated via the computer program). The resonant frequency of the bubble is clearly identified by the scattering values' peak, which then quickly falls off from the maximum due to the effect of the various damping factors, and by the deviation in incident frequency (as defined by wavenumber κ) from resonant frequency.

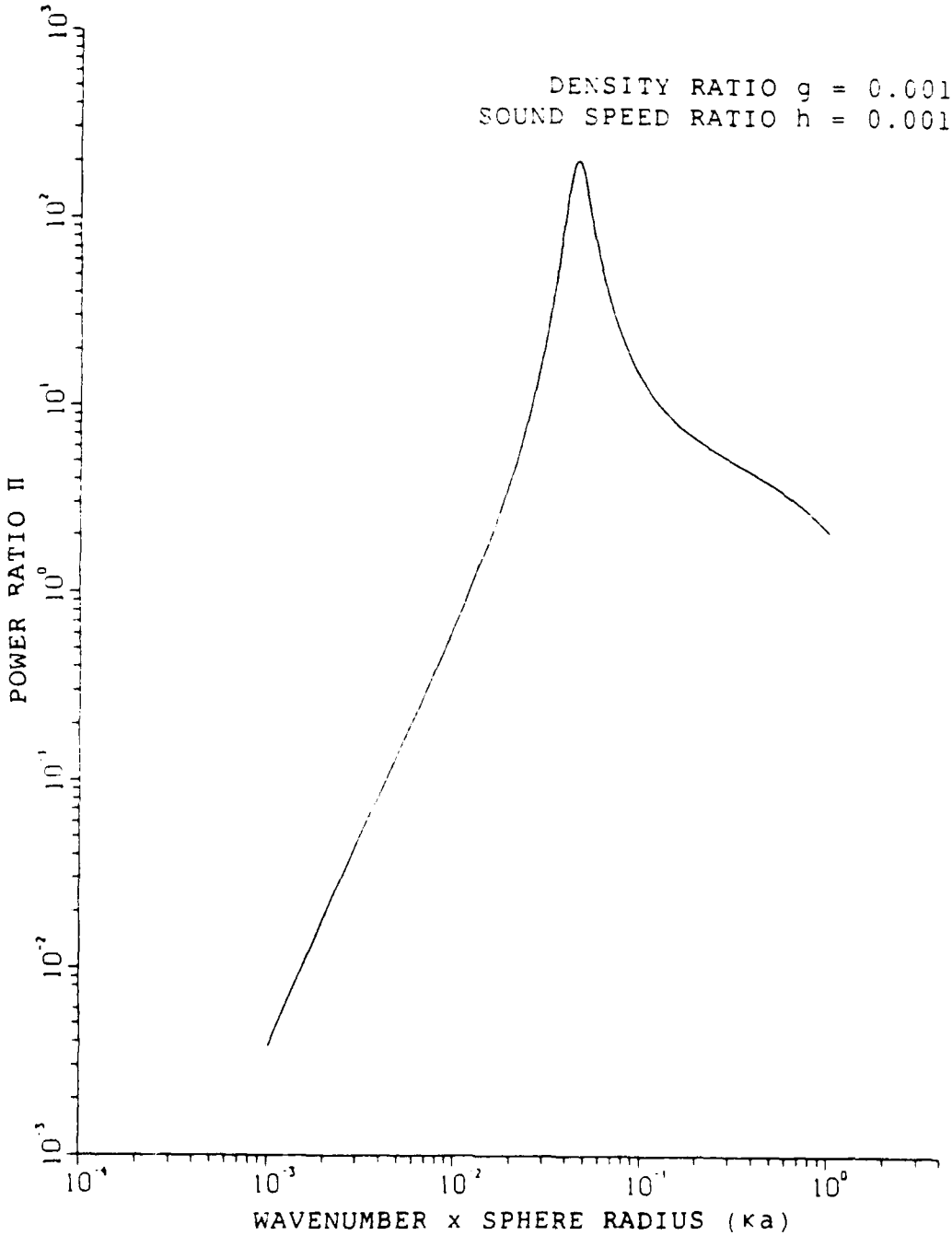

Figure 8. Scattered Power Ratio Π for a Bubble as a Function of Wavenumber x Sphere Radius κa

6. SUMMARY OF PARTICULATE SCATTERING THEORY

Examination of the results of this theoretical scattering model indicates the varying levels of dependence of the scattered wave pressure on sphere and medium parameters, and on incident sound frequency (relative to sphere size), as reflected in the parameter acoustic radius (κa). Figures 3 and 4, presentations of the backscattered reflectivity results for various g and h values, show a greater dependence of R on the sound speed ratio h than on the density ratio g for the ranges tested. As the sound speed of the sphere becomes less than that of the medium ($h < 1$), the backscattered pressure amplitude (figures 3 and 4) and scattered power (figure 5) grow larger than the geometric values ($R > 1$, $\Pi > 1$) for increasing values of κa. For a fluid sphere ($g < 1$, $h < 1$), the magnitude of this backscattered response and the oscillations of the value with increasing sphere size reflect the modal frequencies of the interior waves that have been stimulated in the sphere by the incident wave. For this reason, the reflectivity ratio R for backscattering can be considered to represent the backscattering due to interior resonances (reference 1).

The high interior transmission of the acoustic wave occurs when the sphere is closer to being acoustically "transparent" (reference 2), which is when the sphere is more compressible than the medium ($h < 1$). The presence and magnitude of the generated interior waves are functions of the ratio of the interior acoustic wavelength $\lambda' = 2\pi/\kappa'$ to the sphere radius a, and of the specified density and sound speed values (other possible damping factors have been neglected in the general model). These interior resonances or standing waves in turn scatter and re-scatter the energy generated internally. This concept is again best understood by the continuity relation applied at the sphere boundary, which states that the sum of the incident pressure and the scattered pressure equals the interior pressure.

As a special and extreme case of the fluid sphere, a gas bubble was modeled incorporating the various considerations of damping and resonance factors. Modeling the bubble resonance factor was shown to be a complicated function of the compressibility of the bubble gas; the liquid mass moved by the bubble as it pulsates; the damping factors of the bubble gas, which include consideration of thermal conductivity, shear viscosity, and reradiation effects; the surface tension of the bubble-medium interface; and the heat conducting capability of the bubble. Theoretical scattering results shown for a gas bubble demonstrated the significant acoustic scattering potential for such a compressible sphere (figure 8).

In contrast, for a rigid sphere for which the density and sound speed values are near to or exceed those of the medium ($g > 1$, $h > 1$), there is no interior motion generated or, rather, no enhancement of any interior transmitted energy. Therefore, the reflectivity R can at best approach a uniform value of 1.0 for a larger rigid sphere ($\kappa a > 1$), representing (complete) interception and scattering off the sphere of all incident sound (figure 7).

The plots of figures 2, 3, and 4 clearly show the range of backscattering responses due to interior resonances as a function of the sphere compressibility (fluid versus rigid) and acoustic radius (for the fluid case). As can be noted from figure 3, the backscattered reflectivity value is also affected by a change in the density ratio, increasing for decreasing g value, but on a much smaller scale. This again is logical since a lower g value represents a sphere less dense than the medium and therefore some interior transmission of energy (dependent on h value) occurs. In both cases, the reflectivity approaches a uniform value as g and h increase for $\kappa a > 1$ (references 1 and 2).

The polar plots of figure 2 allow examination of scattering strengths for all values of θ (from large spheres). The density ratio g is held constant at 1.0, which indicates that the medium and sphere fluids are of the same density. Therefore, the scattering patterns generated are due primarily to the difference in sound speed values ($h \neq 1$). This difference in c values causes the incident acoustic waves to be refracted as they hit the sphere, the sound rays bending as they are transmitted through the sphere. Since the dominant effect here is refraction, (the bending of the rays through the sphere), rather than reflection, (the bending back or bouncing of the rays off the sphere), the scattering patterns show much larger forwardscattering than backscattering. (The symmetry of the scattering patterns is due to the assumption of the sphere homogeneity.)

Detailed examination and discussion of these theoretical results are presented by Anderson (reference 2) and in a later review by Clay and Medwin (reference 1), and need not be further discussed here. However, some of the most significant observations from these results, in terms of theoretical scattering magnitudes, are the evidence of reflective and refractive effects dependent on the sphere-to-medium sound speed and density ratios, and the presence of resonance (modal) frequencies in fluid spheres ($g, h < 1$) due to interior wave propagation.

Use of the uniform sphere to model nonspherical, nonuniform particulates has been shown to allow prediction of the scattering response with fair accuracy for small particulates whose dimensions are less than a wavelength, and whose physical parameters are near to those of the medium (reference 1). The next portion of this research will seek to verify this premise and define the accuracy limits of this model by studying available experimental scattering data with respect to the theoretical model just outlined.

parameters are near to those of the medium (reference 1). The next portion of this research will seek to verify this premise and define the accuracy limits of this model by studying available experimental scattering data with respect to the theoretical model just outlined.

APPENDIX
DERIVATIONS OF REFERENCED EQUATIONS

SCATTERING CONSTANTS F_m

Equation (14) from the main text of this report was defined as the incident pressure wave equation, containing the unknown constants F_m:

$$p = P_{inc} \sum_{m=0}^{\infty} F_m P_m(\cos\theta) j_m(\kappa r) e^{-\imath\omega t} \quad .$$

To determine the values of F_m, the Rayleigh equation (reference 6) can be used:

$$e^{\imath\kappa r\cos\theta} = \sum_{m=0}^{\infty} F_m j_m(\kappa r) P_m(\cos\theta) \quad .$$

Letting $\cos\theta = x$, multiplying both sides of the equation by $P_m(x)$, and integrating with respect to x from -1 to 1,

$$\int_{-1}^{+1} P_m(x) e^{\imath\kappa r x}\, dx = \int_{-1}^{+1} \sum_{m=0}^{\infty} F_m j_m(\kappa r) P_m^2(x)\, dx \quad .$$

Rearranging,

$$\int_{-1}^{+1} P_m(x) e^{\imath\kappa r x}\, dx = \sum_{m=0}^{\infty} F_m j_m(\kappa r) \int_{-1}^{+1} P_m^2(x)\, dx \quad .$$

Applying the Legendre principle of orthogonality (references 3 and 6), which states

$$\int_{-1}^{+1} P_m^2(x)\, dx = \frac{2}{2m+1} \quad ,$$

the following simplification is obtained:

$$\int_{-1}^{+1} P_m(x) e^{\imath \kappa r x} \, dx = \sum_{m=0}^{\infty} F_m j_m(\kappa r) \frac{2}{2m+1} .$$

Applying the known spherical Bessel function relation (reference 6) which states

$$j_m(\kappa r) = \frac{1}{2\imath^m} \int_{-1}^{+1} e^{\imath \kappa r x} P_m(x) \, dx ,$$

the final solutions for F_m are obtained:

$$2\imath^m j_m(\kappa r) = F_m j_m(\kappa r) \frac{2}{2m+1} ,$$

$$F_m = (2m + 1)\imath^m .$$

SCATTERING EQUATIONS FOR A BUBBLE

Continuity of Pressure Analysis for Bubble

By examining each of the components of the pressure continuity equation separately, the incident plane wave can first be defined as a uniform wave of given amplitude P_{inc}, varying sinusoidally with time and frequency:

$$p_{inc} = P_{inc} e^{\imath \omega t} . \qquad (A\text{-}1)$$

Similarly, the interior acoustic pressure is a sinusoidal function of time and frequency and unknown amplitude P_{int}:

$$p_{int} = P_{int} e^{\imath \omega t} . \qquad (A\text{-}2)$$

The scattered pressure wave is a spherically-diverging wave, a sinusoidal function of time, frequency, and acoustic radius κa, and of amplitude P_{sc}:

$$p_{sc} = P_{sc}(R_1/R)e^{\imath(\omega t-\kappa a)} \quad , \tag{A-3}$$

These three pressure equations can be combined to expand the given continuity relation (equation (39)) and solve for the interior pressure amplitude P_{int} (at bubble boundary R = a):

$$P_{int} = P_{inc} + \left[P_{sc}\left(\frac{R_1}{a}\right)(1 - \imath\kappa a)\right] - \left(\frac{\mu C_1 u_{sc}}{e^{\imath\omega t_a}}\right) \quad . \tag{A-4}$$

Continuity of Radial Velocity Analysis for Bubble

The governing equation for examining the interior radial velocity of the sound waves for a bubble is derived from the non-adiabatic thermodynamic relation between interior pressure and volume:

$$p_{iT}V^{\gamma(b+\imath d)} = \text{constant} \quad , \tag{A-5}$$

where $p_{iT} = P_{iA} + p_{int}$ is the total interior pressure, γ is the ratio of constant pressure to constant velocity specific heats, and b and d are the constants contributing to the thermal damping definition by modifying γ. $P_{iA} = \beta P_A$, where β is the surface tension compensating factor, and P_A is the exterior hydrostatic pressure (a function of depth).

Equation (A-5) includes modifying parameters to account for the damping due to thermal conductivity and heat conversion in the system, and the surface tension effects influencing the interior pressure. The exponent $\gamma(b+\imath d)$ recognizes that this is (realistically) a non-adiabatic system (defined more explicitly later on). The interior pressure solution for p_{iT} has also been expanded to include the surface tension effects, which increase the given pressure amplitude (P_{int}) in the bubble dramatically, since $P_{iA} >> P_{int}$.

By differentiating equation (A-5) with respect to time, the equation for volume rate of change can be derived and then used to

develop the interior radial velocity equation:

$$\frac{dp_{iT}}{dt} V^{\gamma(b+\imath d)} + p_{iT} \frac{dV^{\gamma(b+\imath d)}}{dt} = 0 ,$$

$$\frac{dV^{\gamma(b+\imath d)}}{dt} = \frac{-V^{\gamma(b+\imath d)}}{p_{iT}} \frac{dp_{iT}}{dt} .$$

Substituting the relation $p_{iT} = P_{iA} + (P_{int}e^{\imath\omega t})$ yields

$$\frac{dV^{\gamma(b+\imath d)}}{dt} = \frac{-V^{\gamma(b+\imath d)}}{[P_{iA}+(P_{int}e^{\imath\omega t})]} \frac{d(P_{iA}+P_{int}e^{\imath\omega t})}{dt} ,$$

$$= \frac{-V^{\gamma(b+\imath d)}}{[P_{iA}+(P_{int}e^{\imath\omega t})]}(0 + \imath\omega P_{int}e^{\imath\omega t}) .$$

Substituting $P_{int}e^{\imath\omega t} = p_{int}$ and recognizing that $P_{iA} >> P_{int}$ gives

$$\frac{dV^{\gamma(b+\imath d)}}{dt} = \frac{-V\gamma(b+\imath d)}{P_{iA}}(\imath\omega p_{int}) .$$

Using the power rule for taking derivatives, which says

$$\frac{d}{dx} u^n = nu^{n-1} \frac{du}{dx} ,$$

gives

$$[\gamma(b+\imath d)]V^{[\gamma(b+\imath d)]-1} \frac{dV}{dt} = \frac{-V^{\gamma(b+\imath d)}}{P_{iA}}(\imath\omega p_{int}) ,$$

$$\frac{dV}{dt} = \frac{-V\imath\omega P_{int}}{P_{iA}\gamma(b+\imath d)} .$$

The radial velocity equation is now developed by substituting

$$dV/dt = 4\pi a^2 u \text{ and } V = (4/3)\pi a^3$$

for a sphere such that

$$4\pi a^2 u = \frac{-\imath\omega P_{int}[(4/3)\pi a^3]}{\gamma(b+\imath d)P_{iA}} .$$

Consequently, the radial velocity for the interior wave is

$$u_{int} = -\imath\omega a P_{int} \frac{e^{\imath\omega t}}{3\gamma(b+\imath d)P_{iA}} , \qquad \text{(A-6)}$$

which is the equation developed by Clay and Medwin (reference 1).

The radial velocity for the scattered wave can be determined more directly by employing the relationship between pressure and radial velocity (acoustic form of Newton's second law) (reference 1):

$$\rho\left(\frac{\partial u}{\partial t}\right) = -\left(\frac{\partial p_{sc}}{\partial R}\right) \qquad \text{at } R = a . \qquad \text{(A-7)}$$

Using the previously defined equation for scattered pressure (equation (A-3)), and incorporating the assumption of $\kappa a << 1$, gives the radial velocity equation for the scattered wave:

$$p_{sc} = P_{sc}(R_1/R)e^{\imath(\omega t-\kappa a)} ,$$

$$= P_{sc}(R_1/a)e^{\imath\omega t}[\cos(\kappa a) - \imath\sin(\kappa a)] .$$

As θ gets very small, $\cos\theta \Rightarrow 1$ and $\sin\theta \Rightarrow \theta$:

$$p_{sc} = P_{sc}(R_1/a)e^{\imath\omega t}(1 - \imath ka) ,$$

$$= [P_{sc}(R_1/a)e^{\imath\omega t}] - [\imath k P_{sc} R_1 e^{\imath\omega t}] .$$

Taking the derivative with respect to a:

$$\frac{\partial p_{sc}}{\partial a} = -\left(\frac{P_{sc}R_1 e^{\imath\omega t}}{a^2}\right) .$$

Substituting this into equation (A-7) gives

$$\frac{\partial u}{\partial t} = \frac{P_{sc}R_1}{\rho a^2} e^{\imath\omega t} .$$

Integrating with respect to time:

$$u = \frac{P_{sc}R_1}{\rho a^2 \imath\omega} e^{\imath\omega t} .$$

Recognizing that $\omega = kc$ and $1/\imath = -\imath$ yields the radial velocity equation for the scattered wave:

$$u_{sc} = -\left(\frac{\imath P_{sc}R_1}{\rho a^2 kc}\right) e^{\imath\omega t} , \qquad \text{(A-8)}$$

which is the equation presented by Clay and Medwin (reference 1).

By equating the radial velocity for the scattered wave (A-8) with that for the interior wave (A-6) in accordance with the continuity equation for radial velocity at the bubble boundary, it is possible to rearrange the parameters and solve for the ratio of interior to scattered pressures:

$$\frac{P_{int}}{P_{sc}} = \frac{3\gamma(b+1d)P_{iA}R1}{\rho c^2 \kappa^2 a^3} \quad . \qquad (A\text{-}9)$$

Setting aside the radial velocity considerations for the moment, it is necessary to examine the resonant frequency for a given bubble. By the definition of resonant frequency for frictionless simple harmonic motion,

$$f_{res} = \omega_{res}/2\pi = (1/2\pi)(s/m)^{\frac{1}{2}} \quad , \qquad (A\text{-}10)$$

where s is the spring force constant, and m is the effective mass of the water moved by the bubble as it oscillates. To solve this equation, it is necessary to determine the values of s and m for the oscillating system. This is achieved by modeling the oscillating bubble system as a spring force system, governed by the Hooke's Law relation (Force = −Spring Constant x Displacement), which can be rewritten for this case as

$$\text{Force} = -\text{Spherical Surface Area} \times \text{Instantaneous Incremental Pressure} \quad ,$$

$$F = (-4\pi a^2)(p_{inst}) \quad . \qquad (A\text{-}11)$$

Therefore, it is first necessary to determine the value of the instantaneous incremental pressure p_{inst}. This is derived from the non-adiabatic thermodynamic relationship between pressure and volume stated earlier as equation (A-5) (variables were defined previously):

$$p_{iT}V^{\gamma(b+1d)} = \text{constant} \quad .$$

Again, this equation includes modifying parameters to account for the damping due to thermal conductivity and heat conversion in the system, and the surface tension effects influencing the interior pressure. Rearranging to solve for the total instantaneous pressure gives

$$p_{iT} = \text{constant}/V^{\gamma(b+1d)} \quad .$$

Taking the derivative to determine the change in total interior pressure with respect to a change in volume:

$$\frac{dp_{iT}}{dV} = -\left[\frac{(\text{constant})[\gamma(b+\imath d)]V^{[\gamma(b+\imath d)]-1}}{V^{2\gamma(b+\imath d)}}\right] . \qquad (A\text{-}12)$$

The change in interior instantaneous pressure with an incremental change in volume (dV) is the instantaneous incremental pressure p_{inst} for the system, defined as follows:

$$dp_{iT} = p_{inst} = p - \beta P_A ,$$

where the β factor accounts for the surface tension effect. The incremental change in the bubble volume can also be expanded:

$$dV = d(4/3\pi a^3) = 4\pi a^2 \xi ,$$

where ξ is the radial displacement of the bubble surface.

Putting these relations back into the equation (A-12), and defining $P_A >> |p_{int}|$, yields the equation for the instantaneous incremental pressure:

$$p_{inst} = -[3P_A\beta\gamma(b + \imath d)\xi]/a . \qquad (A\text{-}13)$$

This solution can now be substituted into equation (A-11) to determine the spring force constant s:

$$F = (-4\pi a^2)(p_{inst}) ,$$

$$F = +12\pi a P_A \beta\gamma(b + \imath d)\xi ,$$

which is in the form $F = -s \times \xi$. Therefore, the spring constant s is determined:

$$s = 12\pi a P_A \beta\gamma(b + \imath d) . \qquad (A\text{-}14)$$

The effective mass m of concern during the bubble oscillations is derived from the equation for the inertial force acting at the bubble surface, which is a function of the scattered pressure value. The effective mass value, which represents the mass of liquid (water) moved by the bubble as it oscillates, works out to be a function of bubble size and water density.

$$m = 4\pi a^3 \rho \quad . \tag{A-15}$$

By using the equations for spring constant s and effective mass m (equations (A-14) and (A-15) respectively), the resonant frequency of a given bubble can now be determined, using equation (A-10):

$$f_{res} = \frac{1}{2\pi a}\sqrt{\frac{3P_A\beta\gamma b}{\rho}} \quad . \tag{A-16}$$

The interior-to-scattered pressure ratio given in equation (A-9) can be rewritten in terms of the resonant-to-incident frequency ratio:

$$f_{inc} = \omega/2\pi = \kappa c/2\pi \ ,$$

$$\frac{f_{res}}{f_{inc}} = \frac{1}{a\kappa c}\sqrt{\frac{3P_A\beta\gamma b}{\rho}} \ ,$$

$$\left(\frac{f_{res}}{f_{inc}}\right)^2 = \frac{1}{a^2\kappa^2 c^2}\,\frac{3P_A\beta\gamma b}{\rho} \ .$$

Substituting this into the pressure amplitude ratio equation (A-9):

$$\frac{P_{int}}{P_{sc}} = \left(\frac{R1}{a}\right)\left(\frac{f_{res}}{f_{inc}}\right)^2\left(1 + \frac{id}{b}\right) \quad . \tag{A-17}$$

By substituting equation (A-17) and the equation for the radial velocity of the scattered wave (equation (A-8)) into the relation derived for the interior pressure amplitude (equation (A-4)), the desired ratio of scattered-to-incident pressure amplitudes can finally be determined:

$$\frac{P_{sc}}{P_{inc}} = \frac{-a/R_1}{[(f_{res}/f_{inc})^2-1]+\imath(\delta)} , \qquad (A\text{-}18)$$

where δ is the damping constant that was defined in equation (42) in the main text of this report. The rest of the (damping) constants used are defined as follows (reference 1):

$$\frac{d}{b} = 3(\gamma-1)\left[\frac{X(\sinh X+\sin X)-2(\cosh X-\cos X)}{X^2(\cosh X-\cos X)+3(\gamma-1)X(\sinh X-\sin X)}\right] ,$$

$$b = \left[1+\left(\frac{d}{b}\right)^2\right]^{-1}\left[1+\frac{3\gamma-1}{X}\frac{\sinh X-\sin X}{\cosh X-\cos X}\right]^{-1} ,$$

$$\beta = 1+\frac{2\tau}{P_A a}\left(1-\frac{1}{3\gamma b}\right) ,$$

$$X = a[(2\omega\rho_{gas}C_{pg})/K_g]^{\frac{1}{2}} ,$$

where $\rho_{gas} = \rho_{ga}[1+2\tau/(P_A a)][1+0.1z]$ is the density of the bubble gas, ρ_{ga} is the density of the free gas at sea level, τ is the surface tension of water-gas interface, $P_A = 1.013*10^6[1+0.1z]$ is the pressure of gas at depth z, C_{pg} is the specific heat at constant pressure of gas, and K_g is the thermal conductivity of the gas.

The scattered-to-incident pressure ratio equation (A-18) can now be used to calculate the total scattering cross section for a gas bubble. The equation for this is shown as equation (41) in the main text of this report.

REFERENCES

1. C.S. Clay and H. Medwin, Acoustical Oceanography: Principles and Applications, John Wiley & Sons, Inc., New York, 1977.

2. V.C. Anderson, "Sound Scattering from a Fluid Sphere," Journal of the Acoustical Society of America, vol. 22, no. 4, 1950.

3. E. Kreyszig, Advanced Engineering Mathematics, Fifth edition, John Wiley & Sons, Inc., New York, 1983.

4. P.M. Morse, Vibration and Sound, McGraw-Hill Book Company, Inc., New York, 1948.

5. P.M. Morse and K.U. Ingard, Theoretical Acoustics, McGraw-Hill Book Company, Inc., New York, 1968.

6. G. Arfken, Mathematical Methods for Physicists, Academic Press, Inc., New York, 1966.

7. R.J. Urick, Principles of Underwater Sound, McGraw-Hill Book Company, Inc., New York, 1975.

INITIAL DISTRIBUTION LIST

Addressee	No. of Copies
CNA	1
DTIC	12